

EFFECTS OF INTERPOLATION ERRORS ON THE ANALYSIS OF DEMs

P. J. J. DESMET

*Laboratory for Experimental Geomorphology, Catholic University of Leuven, Redingenstraat 16, B-3000 Leuven, Belgium**Received 15 December 1995; Revised 23 May 1996; Accepted 12 June 1996*

ABSTRACT

A suite of methods to interpolate a digital elevation model from a ground survey was evaluated with respect to precision and ability to maintain the shape of the original height data. This shape reliability was evaluated by comparing the spatial patterns of secondary terrain parameters derived from the interpolated elevation data. The best interpolation method for this study area was found to be a spline interpolation, which is somewhat contradictory to findings in the literature. The error and uncertainty found in the results for terrain analysis and modelling tools is important and sometimes distressingly high, even for some frequently used local or context operations on altitude. Positional operations, in which the output is determined more by the position in the topographic structure, seem to give more reliable results. Therefore, the results obtained by terrain analysis and spatial modelling need careful interpretation. © 1997 by John Wiley & Sons, Ltd.

Earth surf. processes landf., **22**, 563–580 (1997)

No. of figures: 6 No. of tables: 9 No. of refs: 56

KEY WORDS: digital elevation models; interpolation methods; error propagation; terrain analysis; dynamic modelling

INTRODUCTION

Since their introduction by Miller and Laflamme (1958), digital elevation models (DEMs) have been increasingly used by geomorphologists and hydrologists for mathematical analysis on landscapes and/or modelling of surface processes. A DEM offers the most common method for extracting vital topographic information and even enables the routing of flow across topography (Kirkby, 1990). Topography is a controlling factor in distributed models of landform processes (e.g. Moore *et al.*, 1988, 1993; Dietrich *et al.*, 1993; Engel *et al.*, 1993; Desmet and Govers, 1995) and must be represented as accurately as possible. However, most commercial geographical information system (GIS) packages do not pay any attention to the important issue of DEM quality.

Previous literature on the error in DEMs refers to the effect of the density and distribution of the sample points (Ackermann, 1978; Li, 1988, 1992), to the way in which the data are acquired (Ackermann, 1978; Fryer *et al.*, 1994) and to the characteristics of the terrain (Li, 1992). Little is known about the error occurring during the interpolation. Kubik and Botman (1976) stated that the interpolation accuracy depends primarily on the properties of the surface, on the spacing of the control points, and on the interpolation method itself.

We may state that the interpolation method will influence the derived data from DEMs and the modelling results; however, we do not know to what extent. In this paper, we aim to evaluate the quality of the DEMs generated by a suite of interpolation methods. When evaluating the performance of an interpolation method for terrain analysis and surface process modelling, the DEM has to be evaluated in terms of both 'precision' and 'shape reliability', as accurate interpolators do not necessarily preserve distinct spatial patterns (Declercq, in press). 'Precision' may be defined as the accuracy with which the heights for unsampled points are predicted, and 'shape reliability' as the degree of fidelity with which the shape or the spatial pattern of the topography is maintained in the interpolated surface. We also investigate the effect of errors in height, which may be attributed to interpolation, on a sample of terrain analysis operations in order to see to what extent the interpolation might influence the derived data from DEMs.

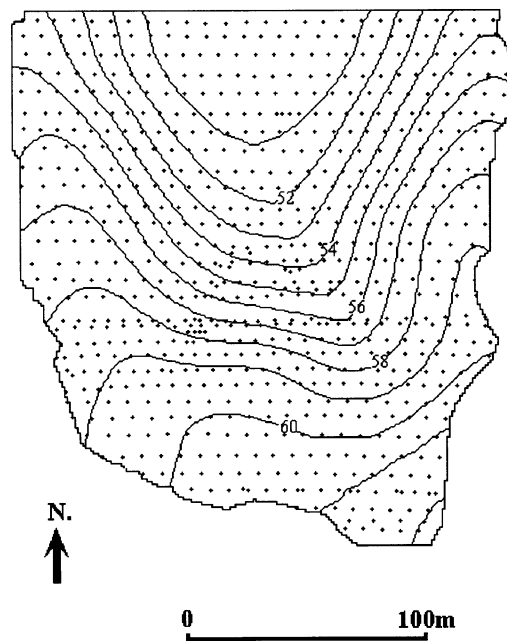


Figure 1. Contour lines for the study area, and the position of the sampled data points (heights in metres)

EXPERIMENTAL DATA

The study area is a small (± 3.5 ha) arable field located in the Belgian Loess Belt. It has an extremely smooth, undulating topography (Figure 1). Such a smooth topography is typical of most of the arable land in western Europe and may be attributed to the smoothing effect of tillage operations. In March 1994, a detailed field survey was set up in order to measure the topography and the gully or rill pattern formed during the previous months. All measurements were taken by using an automatic theodolite. Where necessary, specific points were added; however, as the terrain was very smooth, the finding of specific points was not obvious. A total of 1044 irregularly spaced points was sampled, giving a mean density of ± 300 points ha^{-1} (Figure 1). From these points a grid-based DEM was interpolated. Because of the original objective of the study, a fine resolution of 1 m was required; the density of the sample points enables such a fine grid spacing.

INTERPOLATION METHODS

It is beyond the scope of this paper to give a review of all interpolation methods which can be used to construct a DEM. Therefore, we refer to the work of Rhind (1975), Schut (1976), Lam (1983), Burrough (1986) and Petrie (1990). Here, we present only the methods and modifications used within this study.

The bivariate interpolation offered by the SAS package is, in the terminology of Lam (1983) and Burrough (1986), a piecewise polynomial interpolation. The method is a modification of that described by Akima (1978). It consists of (SAS Institute, 1990):

- dividing the plane into non-overlapping triangles using the positions of the available points;
- fitting a bivariate fifth degree polynomial within each triangle;
- calculating the interpolated values by evaluating the polynomial at each grid point that falls into the triangle.

The coefficients for the polynomial are computed from the values of the function at the vertices of the triangle and from the estimated values for the first and second derivatives of the function at the vertices. The

estimates for these derivatives are computed using n nearest neighbours of the point. We used six nearest neighbours, as for gradually changing data a small number of neighbours is desirable (Declercq, in press). The interpolated surface passes precisely through the sample points. So this method is an exact (Lam, 1983) and local (Burrough, 1986) interpolator. This method will work best for fairly smooth functions with values given at uniformly distributed points in the plane (SAS Institute, 1990).

A modification of the bivariate interpolation is the partial spline interpolation in which a spline is used to estimate the first and second derivatives for the polynomial function. A bivariate spline is fitted to n nearest neighbours and used to estimate the needed derivatives. According to the SAS-GRAPH manual (SAS Institute, 1990), this method produces results that are less smooth than those produced by a global spline interpolation, but smoother than those produced by the default bivariate interpolation.

Spline methods produce a function that passes as close as possible through the data points and still maintains a certain degree of smoothness. The surface generated can be thought of as one that would be formed if a stiff, thin metal plate were forced through or near the given data points. This method results in the determination of an n^3 -order algorithm and is therefore extremely time-consuming for large data sets (Meinguet, 1979; Mitasova *et al.*, 1995). We used the spline function available in the SAS package (SAS Institute, 1990) without extra smoothing. This method can be considered as a simplification of the (thin plate) spline functions used by Mitasova and Mitas (1993), Hutchinson and Gessler (1994) and Hutchinson (1995), and should not be confused with the spline interpolation discussed by Lam (1983) or Burrough (1986), which is a piecewise, local interpolation.

The SAS package also enables a linear interpolation. From the input data points, a set of triangles covering the study area was formed; the height estimates for the unknown grid points were calculated linearly within the overlying triangle. The values lie within the range of the initial values of the vertical variable of the input data set, but the resulting interpolated surface may not be smooth.

A frequently used method is to compute a distance-weighted average value from the local neighbourhood (nearest-neighbour interpolation). As sample points located close together tend to be more alike than observations further away, it seems obvious that the average value should be weighted by a distance factor. Using a narrow neighbourhood and/or assigning a larger importance to the closest neighbours will emphasize local variation; using a broad neighbourhood will produce a smoother output representing the general trend (Burrough, 1986).

The SURFER package (Golden Software, 1989) enables us to choose between a number of distance functions or to use several configurations for the sample data around the unsampled spot. For this study, the reciprocal of the distance was chosen as the weight factor because it gave better results than the inverse of the squared distance. Three divergent configurations for the sample points were taken: four and 12 neighbours randomly spread around the pixel to be interpolated, and 24 neighbours whereby each octant contained three points.

Kriging is essentially a method of estimation by local weighted averaging, but it overcomes several drawbacks of the traditional methods as it provides an optimal interpolation with minimal variances whereby the interpolation weights are determined by the spatial variation of the property to be interpolated and the configuration of the data.

Punctual kriging is an exact interpolator, so the kriged value at a sample point is the measured value there and the variance is zero. However, a map drawn from point estimates in the presence of nugget variance will have discontinuities at the sample points. This can be avoided by computing estimates over (larger) blocks (block kriging) (Burgess and Webster, 1980). We found little difference between punctual and block kriging, but the block estimates may seem more reliable because the estimation variances decrease as the size of the block increases (Burrough, 1986; Oliver and Webster, 1990). Block estimates may also be more realistic since the information for a point is usually intended to represent an area around it.

In this paper, both the determination of the variogram and the kriging interpolation were carried out using GEO-EAS (Englund and Sparks, 1988). This package is found to be very flexible in the search for the best mathematical model describing the variogram, the number of neighbours used for interpolation, and the search for directional effects in the spatial variation. Block kriging with blocks of 2×2 grid cells, with a Gaussian model $\gamma(r) = 1 - \exp(-r^2/a^2)$ (Journel and Huijbregts, 1978) as the stochastic mathematical model for the

variogram, and using six neighbours was found to give the best results. No directional effects were detected.

Some of the interpolation methods did not generate a smooth surface, whereas the real land surface is extremely smooth as it was sculpted by tillage processes and water erosion. Therefore, to get a reliable representation of the topography, the interpolated surface should not be rough. Roughness may be seen as noise due to the interpolation method and may be considered as a criterion for rejecting an interpolation method. This roughness can also be reduced by filtering processes. Two sorts of filtering were carried out on the DEMs originally produced by the linear, bivariate and spline interpolation:

- (1) A mean filter removes some of the angularity or noise and produces a smooth terrain model (Eastman, 1992). This filter calculates new values for each pixel by averaging the old values of a moving window, but is subject to some criticism (Yoeli, 1983; Carter, 1988) as it may remove real local variation. We limited the size of the moving window to 3×3 grid cells.
- (2) The smoothness of the study area has been caused mainly by tillage, a diffusion-type process (Kirkby, 1971; Govers *et al.*, 1994) which can be described by a simple slope-dependent equation. This process will smooth the surface as peaks are eliminated and pits are filled. Applying a diffusion-type model to create a smooth surface is simulating the real process that caused the smoothness. However, this sort of soil redistribution also causes a systematic error: the surface will be lowered on convex (upper) parts and raised on the concave (lower) parts. Two diffusive filters (a weak and a strong one) were applied to both the linear and the default bivariate interpolation.

Few publications have examined the efficiency of various interpolation methods and most refer to a quantitative evaluation of the accuracy. There seems to be a tendency in favour of kriging and distance-weighted methods (Burrough, 1986; van Kuilenburg *et al.*, 1982; Dubrule, 1983, 1984; Oliver and Webster, 1990; Laslett *et al.*, 1987; Declercq, in press), at least for interpolating the spatial variation of soil or hydrological attributes. Lam (1983) does not agree with the use of the distance-weighted methods because she found too many drawbacks. She also rejected the piecewise polynomials, as did Laslett *et al.* (1987). Splines performed reasonably well in the tests of Laslett *et al.* (1987). Burrough (1986) and Oliver and Webster (1990) warned against the use of global methods because of their powerful smoothing and instability due to outliers. Petrie (1990) noted the unpredictable nature of the oscillations when using high-order polynomials. Most of these comparisons were carried out on more or less abruptly changing (soil) data; only Declercq (in press) evaluated the methods for the interpolation of gradually changing data.

PRECISION ASSESSMENT

Two measures are used to evaluate the precision of point interpolations.

- (1) The root mean square error (RMSE) is most commonly used:

$$\text{RMSE} = \sqrt{\frac{\sum_{i=1}^N (Z_{i,\text{observed}} - Z_{i,\text{interpolated}})^2}{N - 1}} \quad (1)$$

where $Z_{i,\text{observed}}$ and $Z_{i,\text{interpolated}}$ represent the measured and interpolated sample point, and N is the number of sample points. The RMSE expresses the degree to which the interpolated value differs from the true value. It is based on the assumption that the errors are random with a mean of zero and are normally distributed around the true value. However, this is not always true (Torlegard *et al.*, 1986; Li, 1988).

- (2) Li (1988) therefore recommended the combination of two other indices:

(i) the mean absolute difference between the interpolated and the true values:

$$\overline{\Delta Z} = \frac{\sum_{i=1}^N |Z_{i,\text{observed}} - Z_{i,\text{interpolated}}|}{N} \quad (2)$$

(ii) the standard deviation of these differences:

$$\rho = \sqrt{\frac{\sum_{i=1}^N (|Z_{i,\text{observed}} - Z_{i,\text{interpolated}}| - \overline{\Delta Z})^2}{N - 1}} \quad (3)$$

As most interpolators are exact, i.e. do not have an error in the sample points, the common practice is to construct two sets of sample points: one set is used for interpolation, the other for validation. The RMSE or mean difference is based on the differences between the predicted and the observed values for the validation set. We performed this cross-validation by omitting respectively 50, 100 and 200 points from the original data set. The precision values for the second case are presented in Table I and are representative for all cross-validations.

The spline interpolation gives the best results for all precision parameters. The bivariate interpolations, both the default and the partial spline, have a higher error but seem to be acceptable as to precision. The linear interpolations and kriging take an intermediate position. The error for the nearest-neighbour interpolations seems large. Surprisingly, a mean filter does not really affect the precision of the interpolation. For the diffusion-type filters some deterioration is observed, but it is not undesirably high.

RELIABILITY OF THE DEMs

The smoothness of the land surface must be represented in the digital representation as this will influence all further analysis and modelling. A visual inspection of the DEMs shows that the nearest-neighbour interpolations yield a stepwise topography (Figure 2). A limited search radius does not fully explain these steps as they were still present when using 24 neighbours, which implies a reasonably large search radius. No visual differences were found between the linear, bivariate and spline interpolations (Figure 2). The partial spline interpolation and kriging cause some artefacts, randomly distributed and at first sight not explainable by the values and configuration of the sample points.

Table I. Accuracy parameters (cm) for the heights (cross-validation based on 100 sample points).

Interpolation method	Mean	Standard deviation	RMSE	Negative maximum	Positive maximum
Linear	4.419	3.250	5.504	-9.301	15.287
Linear/mean filter	4.344	3.216	5.423	-9.177	15.373
Linear/weak diffusive filter	4.377	3.198	5.439	-9.332	15.381
Linear/strong diffusive filter	4.432	3.173	5.470	-9.514	15.411
Bivariate	3.283	2.512	4.147	-9.764	12.466
Bivariate/mean filter	3.254	2.447	4.085	-9.500	12.492
Bivariate/weak diffusive filter	3.310	2.504	4.164	-9.370	12.416
Bivariate/strong diffusive filter	3.323	2.573	4.216	-9.091	12.531
Spline	2.985	2.209	3.726	-8.062	9.491
Spline/mean filter	2.974	2.204	3.714	-7.903	9.510
Block kriging	5.016	4.368	6.671	-19.206	17.640
Partial spline	3.576	2.655	4.469	-10.149	11.697
Nearest neighbour (four random neighbours)	10.342	9.836	14.311	-51.640	39.720
Nearest neighbour (12 random neighbours)	9.424	8.205	12.532	-35.080	37.570
Nearest neighbour (three neighbours/octant)	10.986	9.392	14.497	-27.800	42.770

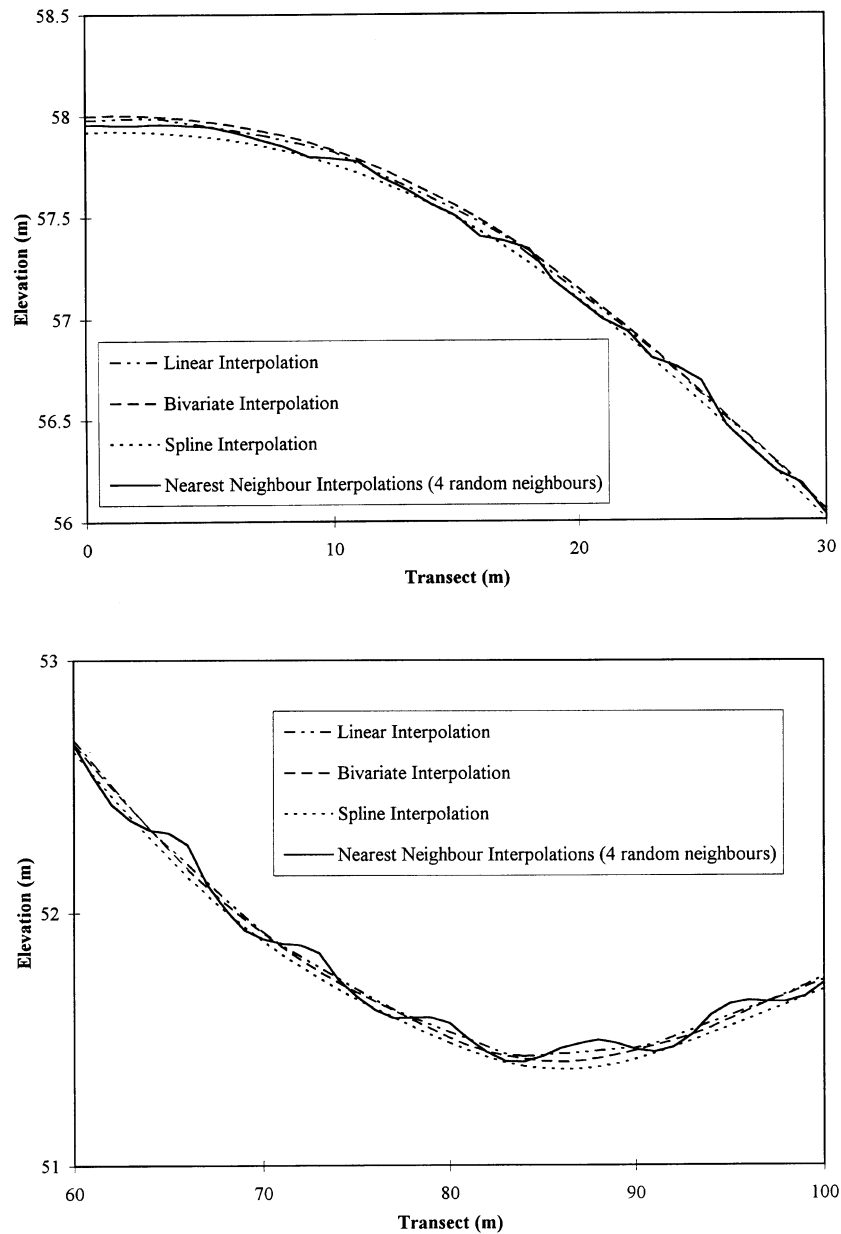


Figure 2. Typical transect through DEM from interfluvium to hollow, taken perpendicular to contour lines

TERRAIN ANALYSIS AND RESULTS

All DEMs were subjected to a sample of frequently used terrain analyses. For this study we selected the calculation of slope gradients, aspect directions, profile curvatures and upslope areas. Afterwards, we implemented a dynamic erosion model to evaluate its sensitivity to error.

Slope gradient

Slope gradient is by far the most frequently used terrain parameter. Its calculation is often possible within a GIS. It is a neighbourhood operator (Burrough, 1986) for which multiple algorithms are available in the

Table II. Moran's I statistic for a sample of terrain analysis tools.

Interpolation method	Slopes	Profile curvatures	Upslope areas	Erosion rates
Linear	0.997	0.394	0.754	0.674
Linear/mean filter	0.999	0.782	0.765	0.738
Linear/weak diffusive filter	0.999	0.587	0.811	0.737
Linear/strong diffusive filter	1.000	0.696	0.834	0.750
Bivariate	0.995	0.019	0.794	0.653
Bivariate/mean filter	0.999	0.761	0.814	0.730
Bivariate/weak diffusive filter	0.999	0.411	0.859	0.739
Bivariate/strong diffusive filter	1.000	0.712	0.889	0.719
Spline	1.000	0.910	0.742	0.742
Spline/mean filter	1.000	0.953	0.831	0.744
Block kriging	0.968	-0.065	0.773	0.128
Partial spline	0.926	0.416	0.774	0.532
Nearest neighbour (four random neighbours)	0.809	0.119	0.696	0.462
Nearest neighbour (12 random neighbours)	0.872	0.241	0.712	0.332
Nearest neighbour (three neighbours/octant)	0.869	-0.065	0.764	0.213

Table III. Some descriptive statistics for the slope gradients (in mm⁻¹).

	Mean	Standard deviation	Minimum	Maximum
Linear interpolation	6.708	3.743	0.112	14.340
Linear interpolation/mean filter	6.698	3.732	0.277	14.301
Linear interpolation/strong diffusive filter	6.681	3.713	0.129	14.130
Bivariate interpolation	6.752	3.787	0.050	17.431
Spline interpolation	6.730	3.772	0.128	14.430
Block kriging	6.822	3.820	0.062	27.438
Nearest neighbour (four random neighbours)	6.931	5.264	0.050	57.368
Nearest neighbour (12 random neighbours)	6.801	4.655	0.016	29.150
Nearest neighbour (three neighbours/octant)	6.488	3.998	0.065	21.704

literature. We used the algorithm presented by Zevenbergen and Thorne (1987). They fitted a second-order polynomial through each 3×3 kernel and found a finite solution for the first derivative of this polynomial. Their solution requires the heights of the four cardinal neighbours.

A smooth surface implies a gradual change of the slope gradients over small distances. This spatial variation can be captured by Moran's I (Moran, 1950) calculated within the IDRISI package (Eastman, 1992), which may be interpreted as a coefficient of spatial autocorrelation with a restricted range between -1 and +1 (Cliff and Ord, 1973). A value near +1 indicates a very strong spatial dependency. The linear, bivariate and spline interpolations yield a high spatial dependency for slopes (Table II), further increased by filtering, especially by the diffusion-type filter. The nearest-neighbour interpolations produce the highest spatial variation; kriging and the partial spline take up an intermediate position.

No major differences are found between the descriptive statistics for the linear, bivariate and spline interpolations (Table III). Filtering decreases the mean, the standard deviation and especially the maximum slope as it smooths the sharp edges. For kriging, the partial spline and nearest-neighbour interpolations, the mean slope, the standard deviation and the maximum slope are considerably higher owing to artefacts, irregularities or the stepwise topography. Increasing the number of neighbours in the interpolation has roughly the same effect as applying a diffusion-type filter or increasing the size of the moving submatrix in the mean filter: heights will be overestimated in concave parts and underestimated in convex parts. This relative smoothing of the overall topography will decrease the mean and maximum slope in particular (Table III).

There is an almost perfect correlation between the slopes for the linear, bivariate and spline interpolations ($R^2 > 0.995$). Filtering the linear and bivariate interpolations even increases the correlation with the spline interpolation. The correlation between the partial spline, kriging and the nearest-neighbour interpolations, and

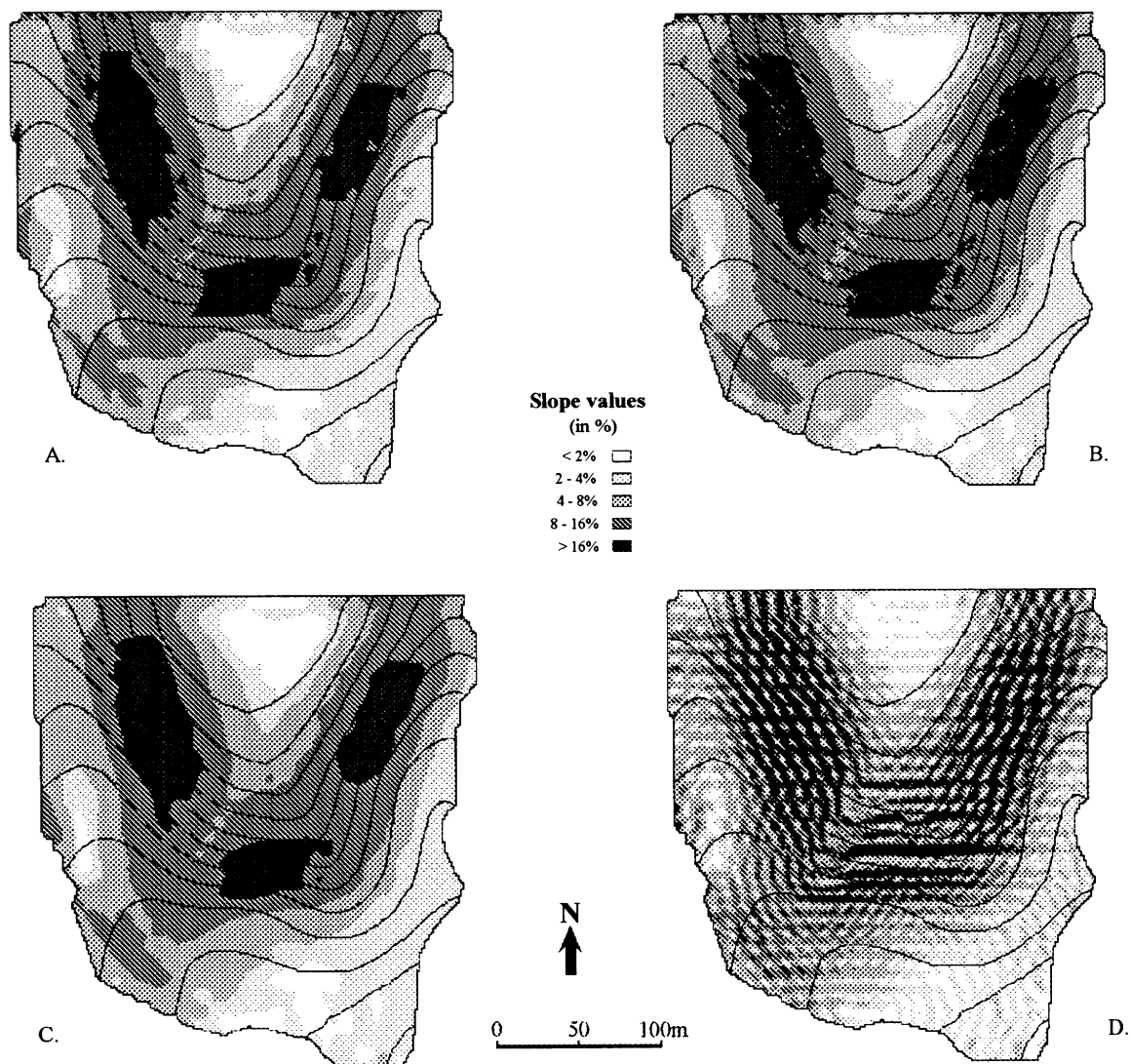


Figure 3. Spatial distribution of slope gradients as a function of the interpolation method: (A) linear interpolation; (B) bivariate interpolation; (C) spline interpolation; (D) nearest-neighbour interpolation with 12 random neighbours. Contour lines from Figure 1 were overlaid for clarity

all others, is poor to moderate ($R^2 < 0.94$ for kriging and < 0.78 for the nearest-neighbour interpolations). Increasing the number of neighbours improves the correlation.

The slope pattern based on the linear interpolation brings the triangles of the original interpolation, which were not visible in the topography, to the fore (Figure 3A). Many tiny pits, produced by the bivariate interpolation, also become visible after the slope calculation (Figure 3B). The spline interpolation yields the most gradual pattern (Figure 3C). The stepwise character of the surfaces produced by all nearest-neighbour interpolations is visible by way of a line structure more or less following the contour lines and bending at the interfluvies (Figure 3D). This is also the case for kriging, although to a lesser degree.

Table IV. Some descriptive statistics for the aspect directions for the subarea (in degrees).

Interpolation method	Mean	Standard deviation	Minimum	Maximum	Range
Linear	332.185	21.749	280.639	388.131	107.492
Linear/mean filter	332.173	21.607	281.263	382.487	101.224
Linear/strong diffusive filter	332.183	21.486	282.242	378.143	95.901
Bivariate	332.147	21.809	277.069	392.558	115.489
Spline	332.108	21.588	280.956	369.991	89.035
Block kriging	332.033	22.929	207.585	462.638	255.053
Nearest neighbour (four random neighbours)	331.313	29.964	202.604	554.262	351.659
Nearest neighbour (12 random neighbours)	331.605	26.758	211.843	540.537	328.693
Nearest neighbour (three neighbours/octant)	331.876	24.375	226.980	407.865	180.885

Aspect direction

The aspect direction or the direction of the steepest slope can be calculated from the height data of a 3×3 kernel (Zevenbergen and Thorne, 1987). The discontinuity at 0 or 360° is a problem for analysis: there is a large mathematical difference between 1 and 359° , but this is not true for the aspect directions. This problem is resolved here by selecting a subarea to limit the range of the data to analyse. The subarea consists of all points having an aspect direction between 0 and 10° or between 280 and 360° for the unfiltered spline interpolation. To avoid the discontinuity, a value of 360° was added to the small angles. This subarea is then used to extract the aspect directions for the other interpolation methods. While the range for the spline interpolation is limited to 90° (i.e. 370 minus 280°), the aberration from this range for the other methods already indicates deviation from the spline interpolation. To compare the ranges, a value of 360° is added to all angles lower than 200° . While the differences in range between the spline interpolation and all linear and bivariate interpolations seem reasonable, the nearest-neighbour interpolation and kriging yield a much larger range, especially when using a small number of neighbours. This points at a significant deviation from the other interpolators (Table IV).

The regression analysis reveals similar conclusions to those for the slope gradients. This is logical as both calculations rely on the first derivative of a fitted surface. However, the correlations are not so good. The analogy with slope gradients is not always true for the spatial patterns: the triangular network typical of the linear interpolation remains visible, especially on the plateaus, as in flat areas small differences in heights cause larger differences in aspect than on steep slopes. The tiny pits for the bivariate interpolations, which are visible in the slope pattern, cannot be seen in the aspect direction pattern. The topographic steps produced by the nearest-neighbour interpolations (including kriging) also cause a line structure in the aspect pattern. A clear differentiation between the flat and the steep parts of the steps is also found.

Profile curvature

Profile curvature describes the rate of change of slope along the line of steepest slope. Similarly to the slope gradient, Zevenbergen and Thorne (1987) proposed a finite solution to calculate the profile curvature from the heights of a 3×3 kernel. As the curvature is the second derivative of the fitted polynomial, this attribute is very sensitive to (abrupt) changes in topography. So, a slow spatial variation of the curvature pattern gives a strong indication of smooth topography, and an irregular spatial pattern indicates topographic roughness. Therefore, curvature may be considered as an appropriate criterion to evaluate some of the interpolation methods for this study area.

Except for the spline interpolation, the spatial dependency of the curvatures is weak for all unfiltered interpolators (Figure 4; Table II). All filters, especially the mean filter, diminish the spatial variation. The almost random variation for kriging and the nearest-neighbour interpolations affirms their inability to be used as appropriate interpolators for the study area. The disturbed patterns we have found for the slope gradients are even more striking for the curvatures (Figure 4D).

Compared to the spline interpolation, the extreme values (maximum concavity and convexity) for the linear and bivariate interpolators without filtering indicate their inadequacy for application to smooth surfaces (Table V). This can only be affirmed by their spatial patterns (Figures 4A, B). As for slope gradients, filtering

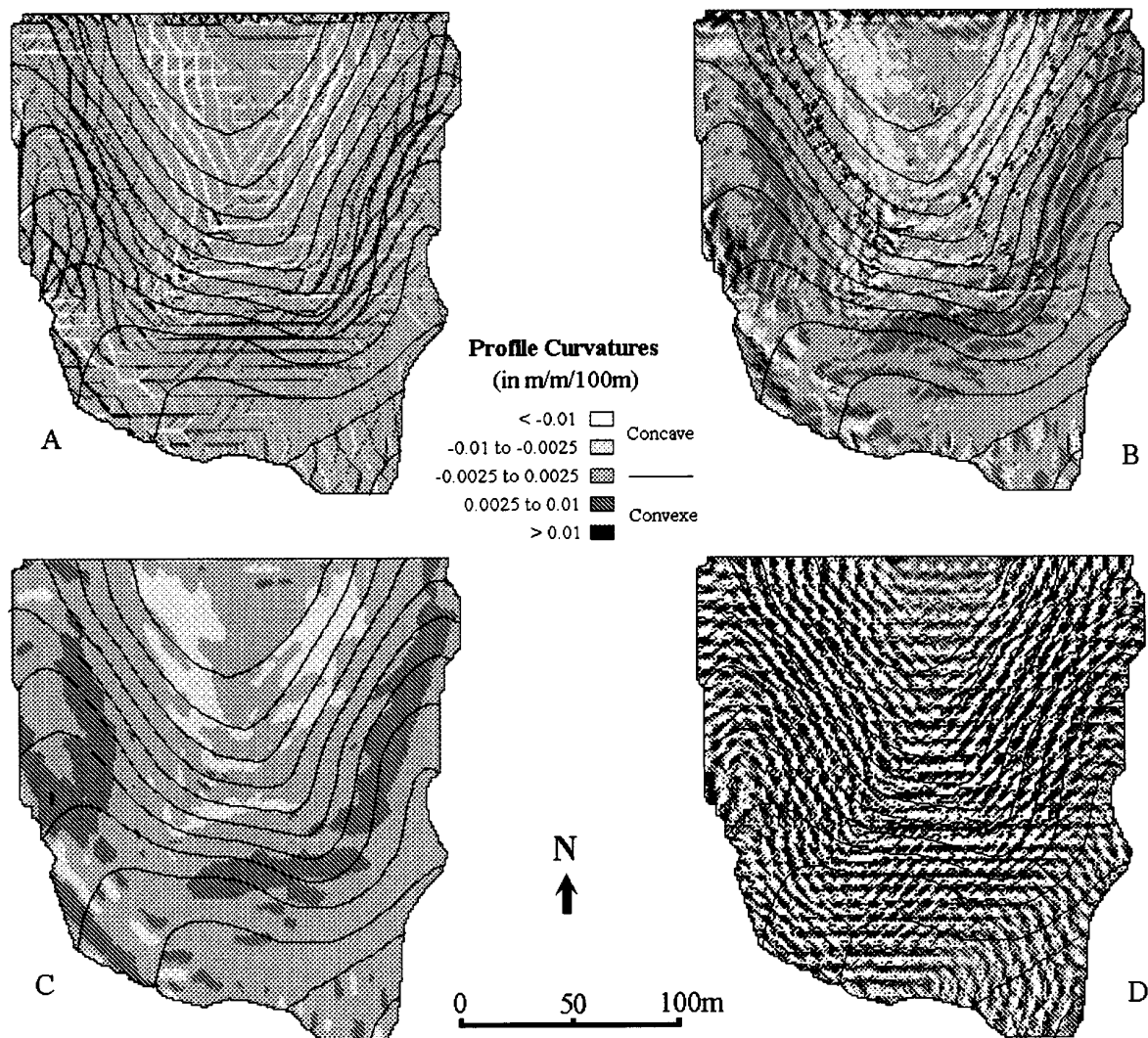


Figure 4. Spatial distribution of the profile curvatures as a function of the interpolation method: (A) linear interpolation; (B) bivariate interpolation; (C) spline interpolation; (D) nearest-neighbour interpolation with 12 random neighbours. Contour lines from Figure 1 were overlaid for clarity

particularly affects the extreme values and may make a linear or bivariate interpolation acceptable. However, it also induces systematic error. The descriptive statistics for the nearest-neighbour interpolators, including kriging, indicate that they are unsuitable for use with smooth topographies (Table V).

Even the correlations between the smooth interpolators (linear, bivariate and spline interpolations) are extremely weak ($R^2 < 0.1$). A strong filter is needed to significantly improve the correlation between the linear or bivariate and the spline interpolation. However, the correlations remain weak ($R^2 < 0.6$).

Upslope drainage area

The upslope (drainage) or contributing area has much potential in terrain analysis (Desmet, 1993; Moore *et al.*, 1993; Desmet and Govers, 1996). It is the total area upslope of a given point or the area contributing to the runoff for this point. Desmet and Govers (1996) demonstrated the similarities and differences between algorithms to calculate the upslope area. Here, we used the flux decomposition algorithm (Desmet and Govers, 1996) in which a vector, directed according to the aspect direction and having a magnitude equal to the upslope

Table V. Some descriptive statistics for the curvatures (in m m^{-1} per 100 m).

	Mean	Standard deviation	Minimum	Maximum
Linear interpolation	0.0358	0.531	-10.280	7.173
Linear interpolation/mean filter	0.0354	0.330	-3.568	2.770
Linear interpolation/strong diffusive filter	0.0362	0.280	-2.815	4.502
Bivariate interpolation	0.0309	0.809	-18.993	9.367
Spline interpolation	0.0307	0.264	-3.965	2.281
Block kriging	0.0363	2.097	-54.772	36.710
Nearest neighbour (four random neighbours)	0.0217	5.484	-54.410	66.871
Nearest neighbour (12 random neighbours)	0.0241	3.547	-20.509	25.052
Nearest neighbour (three neighbours/octant)	0.0232	4.222	-25.950	20.753

Table VI. Some descriptive statistics for the upslope areas (in m^2).

	Mean	Standard deviation	Minimum	Maximum
Linear interpolation	94.81	362.43	0.5	11821.7
Linear interpolation/mean filter	94.47	353.08	0.5	10762.4
Linear interpolation/strong diffusive filter	94.02	320.76	0.5	7477.92
Bivariate interpolation	95.67	340.24	0.5	10936.0
Spline interpolation	94.64	354.98	0.5	10061.4
Block kriging	72.48	235.23	0.5	7529.00
Nearest neighbour (four random neighbours)	55.31	101.20	0.5	3703.38
Nearest neighbour (12 random neighbours)	54.09	101.68	0.5	5406.01
Nearest neighbour (three neighbours/octant)	91.41	289.96	0.5	7394.33

area to be distributed, increased with the area of the grid cell itself, is split into its two ordinal components.

No striking differences can be found between the descriptive statistics for the smooth interpolators (Table VI). Filtering decreases the standard deviation and especially the maximum upslope area as filtering causes a greater potential for divergent flow. An increased divergence also increases the mean value. Owing to a number of artefacts, flow is frequently blocked leading to a lower mean and maximum for the 'rough' (nearest-neighbour, kriging and partial spline) interpolators.

There is a reasonably good correlation between the upslope areas for the unfiltered linear, bivariate and spline interpolations ($R^2 > 0.85$). Filtering the linear or bivariate interpolation improves the correlation with the spline interpolation. The regression between the 'rough' interpolators and the others is moderate to poor ($R^2 < 0.53$). Increasing the number of neighbours involved in the interpolation improves the correlation with the smooth interpolators.

The upslope area for a smooth topography increases gradually downslope, so the spatial variation has to be limited. This is only found for the spline interpolation (Figure 5C; Table II). For the bivariate interpolation the pattern is disturbed by some local accumulations due to the tiny pits (Figure 5B), and for the linear interpolation by triangular offshots (Figure 5A). The steps produced by the nearest-neighbour interpolations cause local accumulations of flow along, and sometimes breaking through, the steps, resulting in small erratic and frequently blocked drainage lines oriented along and perpendicular to the contour lines (Figure 5D). A similar, but less regular pattern is found for kriging.

In a number of hydrological models (e.g. Young *et al.*, 1989; Engel *et al.*, 1993) the direction of the steepest slope is used to determine the flow direction: the neighbour that the direction of the steepest slope points to becomes the destination of the flow. Height differences may cause significant differences in the direction of the steepest slope; these are greatest in flat areas (Chang and Tsai, 1991; Carter, 1992; Heuvelink, 1993) and can lead to a deviation in flow direction. Table VII gives the percentage of pixels which agree in flow direction for each pair of interpolation methods. The agreement between the linear, bivariate and spline interpolations is not very high. Filtering will increase the correspondence as this implies an evolution of the topography in the same sense. The correspondence between the nearest-neighbour and the smooth interpolators is distressingly bad. Kriging and the partial spline interpolation again take an intermediate position.

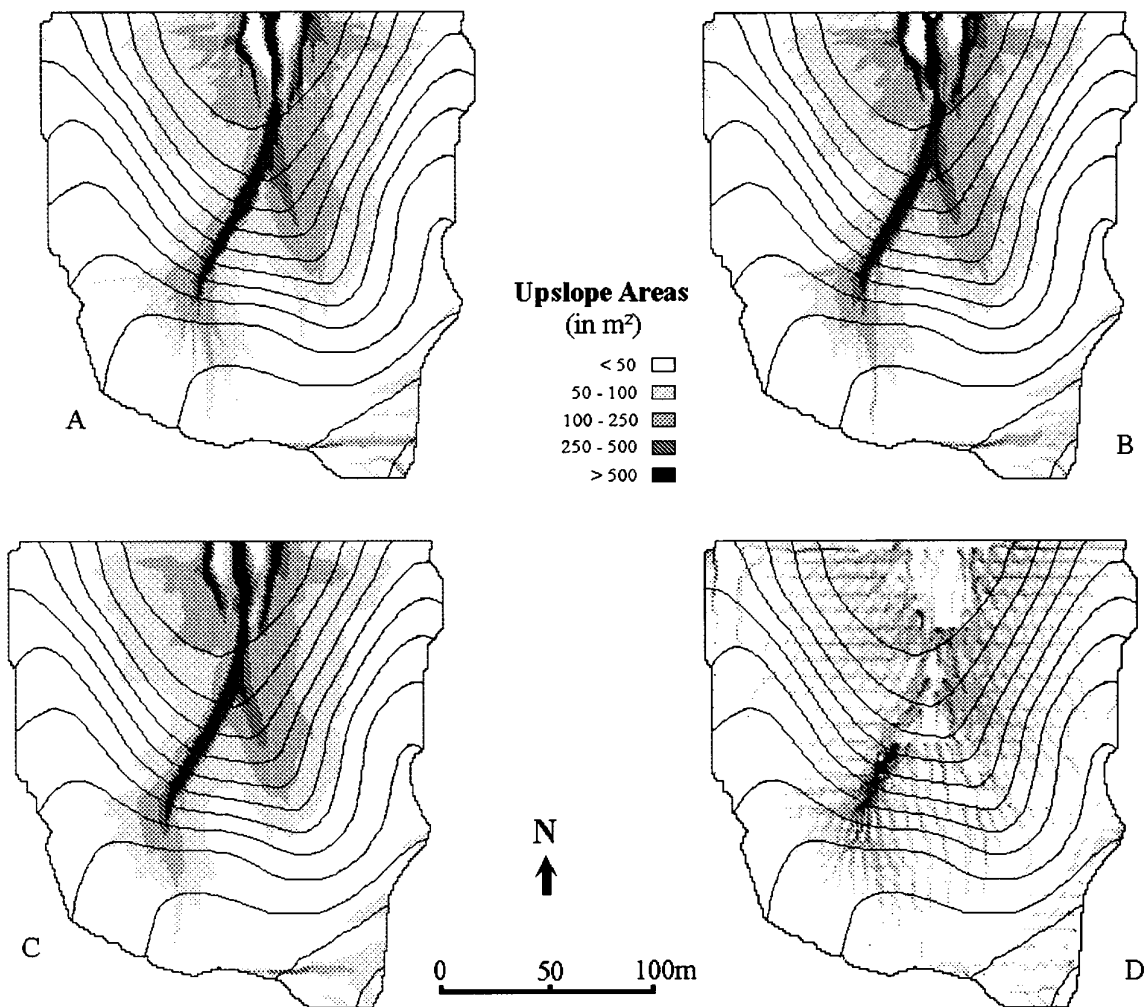


Figure 5. Spatial distribution of the upslope areas as a function of the interpolation method: (A) linear interpolation; (B) bivariate interpolation; (C) spline interpolation; (D) nearest-neighbour interpolation with 12 random neighbours. Contour lines from Figure 1 were overlaid for clarity

Dynamic erosion modelling

In addition to these topographic attributes, we were interested to know how topographic errors affect the modelling of geomorphological or hydrological processes. For this purpose we used the general formulation of the sediment transport rate along a hillslope as proposed by Kirkby *et al.* (1987). This formulation, which accounts for both overland flow and diffusion-type processes, provides a useful basis for erosion simulation:

$$Q_s = k_2 \left[1 + \left(\frac{x}{u} \right)^2 \right] S \quad (4)$$

where Q_s = the sediment transport flux ($\text{kg m}^{-1} \text{a}^{-1}$), x = the distance from the divide (m), S = the local slope gradient (m m^{-1}), k_2 = the diffusion constant ($\text{kg m}^{-1} \text{a}^{-1}$), and u = the distance beyond which the overland flow term becomes larger than the diffusion term (m). This equation uses only two influencing variables: slope gradient and slope length. To expand this equation for use with catchments, slope length has to be replaced by the unit upslope area, i.e. the upslope area per unit of contour length (Ahnert, 1976; Desmet and Govers, 1995).

Table VII. Agreement (in %) in flow directions based on the direction of the steepest slope.

	Bivariate	Kriging	Spline	Partial spline	Nearest neighbour (four random neighbours)	Nearest neighbour (three neighbours/ octant)
Linear	91.3	86.1	92.6	86.4	68.4	73.7
Bivariate		86.7	94.1	88.7	67.7	72.3
Kriging			87.5	83.6	64.2	70.1
Spline				88.6	68.7	72.9
Partial spline					65.8	70.3
Nearest neighbour (four random neighbours)						59.6

Table VIII. Some descriptive statistics for the erosion values (in cm).

	Mean	Standard deviation	Minimum	Maximum
Linear interpolation	-0.140	1.423	-27.91	7.06
Linear interpolation/mean filter	-0.112	1.032	-22.09	4.83
Linear interpolation/strong diffusive filter	-0.113	0.940	-19.66	3.68
Bivariate interpolation	-0.107	1.169	-23.27	12.08
Spline interpolation	-0.103	1.010	-22.51	4.55
Block kriging	-0.149	7.181	-462.98	358.85
Nearest neighbour (four random neighbours)	-0.063	9.009	-100.64	96.26
Nearest neighbour (12 random neighbours)	-0.171	6.992	-231.39	206.82
Nearest neighbour (three neighbours/octant)	-0.162	6.180	-324.33	296.96

For a two-dimensional topography, Govers *et al.* (1996) extended Equation 4 to:

$$Q_s = k_2 \left[S + \frac{k_1}{(n+1)k_2} S^m A_s^{n+1} \right] \quad (5)$$

where A_s = unit upslope area ($\text{m}^2 \text{m}^{-1}$) and k_1, k_2, m, n = constants. In this formulation the slope and upslope area effect on overland flow erosion can be assessed by modifying m and n , respectively. More details about the model implementation can be found in Govers *et al.* (1996).

Instead of using one steady-state value for the unit upslope area, we employed what may be called an 'areagram'. An areagram represents the amount of unit upslope area per virtual unit of time passing through a grid cell. The integration of the areagram function yields the total unit upslope area. The areagram was calculated as follows. First, a value representing the grid cell area was attributed to each cell. Then, this amount was distributed over the surface following an adopted flow routing algorithm. In a single time step, the flow and sediment were simply routed from a cell to one or more of its downslope neighbours, thus neglecting variation in flow velocities due to discharge and slope. This approach can be seen as an intermediate solution between simply using the upslope area and a full hydrologic routing of sediment and water. So, Equation 5 is changed to:

$$q_{s,t=t_i} = k_2 \left[S + \frac{k_1}{(n+1)k_2} S^m a_{s,t=t_i}^{n+1} \right] \quad (6)$$

where :

$$E = \nabla Q_s = \int_{t_i=1}^T \nabla q_{s,t=t_i} dt = \text{erosion (in kg m}^{-2}\text{)}$$

$$A_s = \int_{t_i=1}^T a_{s,t=t_i} dt = \text{total unit upslope area (m)}$$

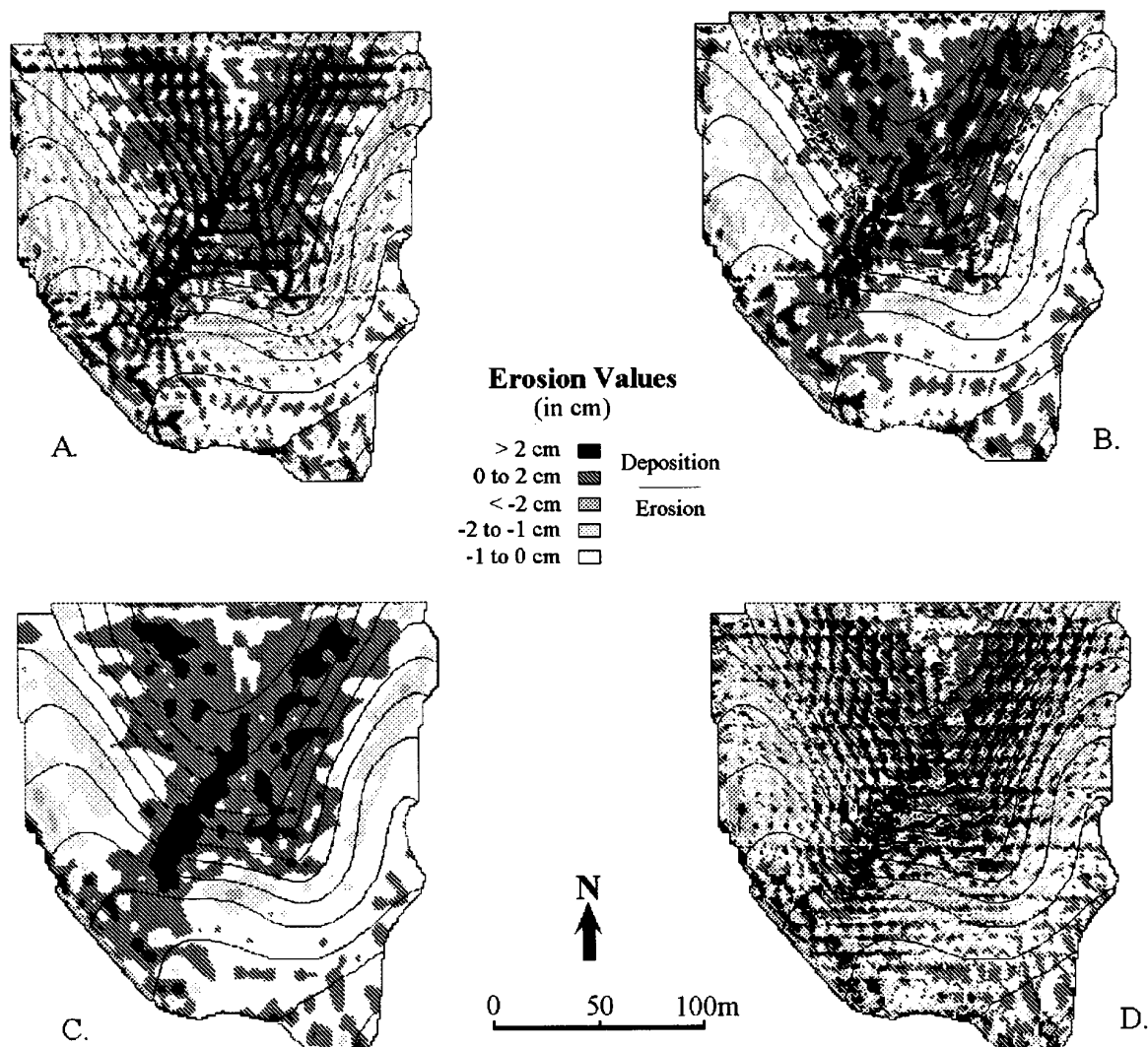


Figure 6. Erosion patterns as a function of the interpolation method: (A) linear interpolation; (B) bivariate interpolation; (C) spline interpolation; (D) nearest-neighbour interpolation with 12 random neighbours. Contour lines from Figure 1 were overlaid for clarity

and t_1 = virtual unit of time. Equation 6 was implemented in a computer program which was run three times, each run consisting of 300 time units (i.e. parameter T). The values for the constants used were: $k_1 = 40$; $k_2 = 2$; $m = 1.45$; $n = 0.75$. These constants were derived from literature and yield erosion patterns consistent with observations on arable land in Belgium where both water and tillage erosion occur (Govers *et al.*, 1994).

The descriptive statistics, given in Table VIII, seem to be strongly influenced by the smoothness of the topography; rough topographies cause suspiciously high maximum erosion and deposition rates, sometimes more than a few metres, whereas these maxima reach only a few centimetres for smooth surfaces. However, even on relatively smooth surfaces, tiny pits or small irregularities may cause a distortion of the normal rates. This also implies that the correlations between the unfiltered smooth interpolators are fairly bad ($R^2 < 0.6$) and that a filtering of the linear or bivariate interpolation is needed to improve the correlation with the spline interpolation.

The spatial variation of the erosion data is rather limited for smooth surfaces and will further decrease after filtering the DEM (Table II). The results for the rough interpolators are much more spatially random, as the patterns from diffusive modelling are strongly influenced by the local variation in slope, i.e. curvature (Govers *et al.*, 1996). The anticipated pattern of erosion on the convex interfluvies and upper slopes, and deposition on

the concave lower slopes and hollows is found for the spline interpolation (Figure 6C). The triangular structure and the tiny pits for, respectively, the linear and bivariate interpolations cause a local alternation of erosion and deposition (Figures 6A, B). Moreover, their pattern is patchy owing to invisible irregularities. The erosion pattern for kriging and the nearest-neighbour interpolation is fully influenced by the curvature pattern, i.e. alternating lines of erosion and deposition parallel to the contour lines (Figure 6D). The erosion lines become relatively stronger further upslope, and vice versa.

DISCUSSION

Choice of interpolation method

Based on the topographic artefacts we found, it is clear that, at least for this study area, we have to reject kriging and the nearest-neighbour interpolations, both of which are distance-weighted methods. This might seem strange as in the literature kriging is referred to as an optimal interpolator (e.g. Burrough, 1986; Oliver and Webster, 1990), at least for the interpolation of 'invisible' soil parameters. Others (e.g. van Kuilenburg *et al.*, 1982; Declercq, in press) considered the nearest-neighbour interpolation as appropriate.

The topographic steps caused by these interpolators remain present even after using 24 neighbours and changing the search sector. A further increase of the number of neighbours might decrease the artefacts, but will further affect the quality of the DEM (Table I). As these steps are approximately parallel to the contour lines, they did not seem to be caused by the configuration of the sample points.

The choice of the appropriate interpolation method for terrain analysis is a compromise between precision and shape reliability. The cross-validations and the terrain analyses to evaluate the shape reliability point to the same conclusion: the spline interpolation is the most appropriate interpolator for this study area. We have to be cautious in extrapolating this conclusion as the study area has an extremely smooth topography; for an irregular, rough topography splines might not fully capture local variation. According to Li (1994) there is also a relationship between the accuracy of the DEM and the configuration of the sample points. Our sample points were more or less regularly spaced (Figure 1), a configuration that did not perform badly in the study of Li (1994). On the other hand, these remarks do not invalidate the results we derived with respect to the sensitivity of topographic differences on terrain analysis and spatial modelling.

Sensitivity of terrain analysis

In order to evaluate the sensitivity of terrain analysis to the topographic input, we might compare the differences between the 15 topographic input files to the differences between the 15 output files. This can be achieved by calculating the mean pixel-wise standard deviation, both for the input and the output files. The pixel-wise standard deviations were calculated based on the 15 values for each pixel. While the pixel-wise standard deviation is a measure of dispersion for the 15 pixel values, the mean pixel-wise standard deviation, calculated as the mean of all pixel-wise standard deviations within the study area, can be considered as a measure for the differences between the 15 files. A comparison between the mean pixel-wise standard deviations for the topographic input files and for the output files may then give an indication of the sensitivity of the terrain analysis tool to topographic errors; a relatively high value for the output files means a high sensitivity to topographic errors.

It should be borne in mind that the mean pixel-wise standard deviation only gives a mean measure of dispersion between the 15 files and tells nothing about the spatial variability of the dispersion. The standard deviation of the pixel-wise standard deviations may be used as a measure for the variation of the pixel-wise standard deviations.

If the output values imply an order, the mean pixel-wise standard deviation has to be replaced by the mean pixel-wise coefficient of variation which is calculated in an analogous way. This is true for most analyses. As the error in height or aspect direction is assumed to be independent of the height or aspect itself, the mean pixel-wise standard deviation is used for these parameters. The results are summarized in Table IX; all statistics were calculated using the 15 available (input or output) files.

Elevations. The mean variation between the 15 topographical surfaces (i.e. 2.8 cm) is relatively large. This is

Table IX. Standard deviations and coefficients of variation for the input and resulting files.

	Mean pixel-wise standard deviation	Standard deviation of the pixel-wise standard deviations	Mean pixel-wise coefficient of variation (%)	Standard deviation of the pixel-wise coefficients of variation (%)
Elevation	2.86	2.43	0.0513	0.043
Slope gradient (%)	1.12	1.16	18.28	18.327
Steepest descent (%)	1.30	1.27	21.27	18.898
Profile curvature (%/100m)	1.72	1.33	1600	71069
Aspect directions (°)	6.71	4.50	2.02	1.303
Upslope areas (m ²) – flux decomposition	35.35	157.71	30.07	23.656
Upslope areas (m ²) – steepest descent direction	82.91	362.28	101.48	58.106
Kirkby model (cm)	2.503	7.417	1806	722421

mainly due to the distance-weighted methods. These standard deviations are also spatially dependent: the linear middle slopes generally show lower standard deviations than the curved upper and lower slopes.

Slope gradients. The slope gradients are relatively sensitive to differences in the input; a mean variation of about 18 per cent between the slope files means a significant propagation of the differences in topography. Calculation of the steepest descent is frequently used to assign the slope gradient to a grid cell. This method needs the height of only one neighbouring point and is, as Table IX illustrates, a little more sensitive to error in height.

Curvatures. The curvatures are very sensitive to error. As curvatures are the second derivatives of the surface, their calculation implies an intensification of the sensitivity to error. The uncertainty associated with curvatures seems dangerous as this result may not only be attributed to the rough interpolators.

Aspect directions. As for slope gradients, aspect directions are calculated as the first derivative of the surface; a similar sensitivity may therefore be expected. This similarity is difficult to assess as we have to use the standard deviations. However, our data (e.g. the regressions, which are slightly worse) do not contradict results from other studies, which concluded that the aspect calculation is slightly more sensitive to errors than the slope gradients (Chang and Tsai, 1991; Carter, 1992).

Upslope areas. Surprisingly, the sensitivity of upslope areas to topographic differences is relatively moderate. The coefficients of variation suggest that the flux decomposition algorithm provides a robust way of calculating the upslope area. The frequently used steepest descent algorithm (e.g. Jenson and Domingue, 1988; Morris and Heerdegen, 1988; Panuska *et al.*, 1991), in which the upslope area present in a point is directed towards the neighbour having the steepest downslope path, is far more sensitive to error (Table IX). The higher mean pixel-wise coefficient of variation for this algorithm is a systematic phenomenon, not caused by a few outliers. This is in full agreement with a conclusion reached by Desmet and Govers (1996), who point to the high sensitivity of this method to topographic error.

Erosion values. The Kirkby erosion model is extremely sensitive to topographic differences. This is not unexpected as curvature is a determining factor for this transport-limited erosion model. Decreasing the relative contribution of water erosion in the flux (i.e. a lower k_1 value in Equation 6) increases the sensitivity, and vice versa. This type of model is also far more sensitive to topographic error than a detachment-limited water erosion model as presented by Desmet and Govers (1995), where patterns are determined more by position and less by the local context.

CONCLUSIONS

A suite of interpolation methods to construct a digital elevation model from irregularly spaced sample points has been evaluated with regard to precision and ability to maintain the shape of the original height data. The shape reliability is studied by comparing the spatial patterns of the output obtained by applying a set of terrain analysis and modelling tools on the interpolated elevations.

The spline interpolation yielded the best results as to both precision and shape reliability for the study area,

which is somewhat contradictory to findings in the literature. The extrapolation of this conclusion must be done with care as the study area was extremely smooth.

The sensitivity of topographic differences (due to interpolation) on terrain analysis is important. The relative differences in the input increase by one or more orders of magnitude after terrain analysis, also causing systematic patterns. Positional attributes, in which the output is determined more by the position in the topographic structure, seem to give reliable results. Context operators, which are generally accepted and frequently used in commercial GIS packages, are more sensitive: even the slope gradients, which only imply a simple calculation, are almost as sensitive as the upslope drainage areas. For curvatures or for the Kirkby erosion model (results of which are surely not only dependent on position) the uncertainty is dramatic.

Eight of the 15 interpolation methods were filtered modifications of basic methods and thus represent adjustments into the same direction, i.e. smoothing. We may therefore expect a still higher sensitivity when only the basic (unfiltered) interpolation methods are used. This emphasizes the care with which the interpolation method has to be chosen, and with which results from terrain analysis and spatial modelling have to be interpreted.

ACKNOWLEDGEMENTS

The author wishes to thank Dr F. Declercq for discussing the interpolation methods and software, Dr J. Poesen and Dr G. Govers for useful comments and help in the field, and Mr L. Cleeren, Mr D. Grobben and Mr K. Toebat for help in the field. Financial support from the European Community is also acknowledged. This manuscript was much improved thanks to the comments of two anonymous referees.

REFERENCES

- Ackermann, F. 1978. 'Experimental investigation into the accuracy of contouring from DTM'. *Photogrammetric Engineering and Remote Sensing*, **44**(12), 1537–1548.
- Ahnert, F. 1976. 'Brief description of a comprehensive three-dimension process–response model of landform development', *Zeitschrift für Geomorphologie, Suppl. Band*, **25**, 29–49.
- Akima, H. 1978. 'A method of bivariate interpolation and smooth surface fitting for irregularly distributed data points', *ACM Transactions on Mathematical Software*, **4**(2), 148–159.
- Burgess, T. M. and Webster, R. 1980. 'Optimal interpolation and isarithmic mapping. 1. The semi-variogram and punctual kriging', *Journal of Soil Science*, **31**, 315–332.
- Burrough, P. A. 1986. *Principles of Geographical Information Systems for Land Resources Assessment*, Clarendon Press, Oxford, 194 pp.
- Carter, J. 1988. 'Digital representations of topographic surfaces', *Photogrammetric Engineering and Remote Sensing*, **54**(11), 1577–1580.
- Carter, J. 1992. 'The effect of data precision on the calculation of slope and aspect using gridded DEMs', *Cartographica*, **29**(1), 22–34.
- Chang, K. and Tsai, B. 1991. 'The effect of DEM resolution on slope and aspect mapping', *Cartography and Geographic Information Systems*, **18**(1), 69–77.
- Cliff, A. D. and Ord, J. K. 1973. *Spatial Processes – Models and applications*, Pion, London, 261 pp.
- Declercq, F. (in press). 'Interpolation methods for scattered sample data: accuracy, spatial patterns, processing time', *Cartography and Geographic Information Systems*.
- Desmet, P. J. J. 1993. 'The use of digital elevation models in geomorphology', *Tijdschrift voor Belg. Ver. Aandr. Studies, BEVAS*, **62**(1), 47–66.
- Desmet, P. J. J. and Govers, G. 1995. 'GIS-based simulation of erosion and deposition patterns in an agricultural landscape: a comparison of model results with soil map information', *Catena*, **25**, 389–401.
- Desmet, P. J. J. and Govers, G. 1996. 'Comparison of routing algorithms for digital elevation models and their implications for predicting ephemeral gullies', *International Journal of Geographical Information Systems*, **10**, 311–331.
- Dietrich, W. E., Wilson, C. J., Montgomery, D. R. and McKean, J. 1993. 'Analysis of erosion thresholds, channel networks, and landscape morphology using a digital terrain model', *The Journal of Geology*, **101**, 259–278.
- Dubrulle, O. 1983. 'Two methods with different objectives: splines and kriging', *Mathematical Geology*, **15**, 245–255.
- Dubrulle, O. 1984. 'Comparing splines and kriging', *Computers and Geosciences*, **10**(2), 327–338.
- Eastman, R. 1992. *Idrisi version 4.0, Technical Reference*, Clark University, Graduate School of Geography, Worcester, Mass., 202 pp.
- Engel, B. A., Srinivasan, R. and Rewerts, C. 1993. 'A spatial decision support system for modelling and managing agricultural non-point-source pollution', in Goodchild, M. F., Parks, B. O. and Steyaert, L. T. (Eds), *Environmental Modelling with GIS*, Oxford University Press, New York, 231–237.
- Englund, E. and Sparks, A. 1988. *GEO-EAS User's Guide*, Environmental Monitoring Systems Laboratory Research and Development, US Environmental Protection Agency, Las Vegas, Nevada, USA.
- Fryer, J. G., Chandler, J. H. and Cooper, M. A. R. 1994. 'On the accuracy of heighting from aerial photographs and maps: implications to process modellers', *Earth Surface Processes and Landforms*, **19**, 577–583.
- Golden Software, 1989. *SURFER Version 4. Reference Manual Volume 1*, Golden Software Inc., Colorado.

- Govers, G., Vandaele, K., Desmet, P. J. J., Poesen, J. and Bunte, K. 1994. 'An investigation of the role of soil tillage in soil redistribution on hillslopes', *European Journal of Soil Science*, **45**, 469–478.
- Govers, G., Quine, T. A., Desmet, P. J. J. and Walling, D. E. (1996). 'The relative contribution of soil tillage and overland flow erosion to soil redistribution on agricultural land', *Earth Surface Processes and Landforms*, **21**, 929–946.
- Heuvelink, G. B. M. 1993. *Error Propagation in Quantitative Spatial Modelling*, KNAG Utrecht, 151 pp.
- Hutchinson, M. F. 1995. 'Interpolating mean rainfall using thin plate smoothing splines', *International Journal of Geographical Information Systems*, **9**(4), 385–403.
- Hutchinson, M. F. and Gessler, P. E. 1994. 'Splines – more than just a smooth interpolator', *Geoderma*, **62**, 45–67.
- Jenson, S. K. and Domingue, J. O. 1988. 'Extracting topographic structure from digital elevation data for geographic information system analysis', *Photogrammetric Engineering and Remote Sensing*, **54**(11), 1593–1600.
- Journel, A. J. and Huijbregts, C. J. 1978. *Mining Geostatistics*, Academic Press, London, 600 pp.
- Kirkby, M. J. 1971. 'Hillslope process–response models based on the continuity equation', in Brunsden D. (Ed.), *Hillslopes: Form and Process*, Institute of British Geographers Special Publication, **3**, 15–30.
- Kirkby, M. J. 1990. 'The landscape viewed through models', *Zeitschrift für Geomorphologie, Suppl. Brand*, **79**, 63–81.
- Kirkby, M. J., Naden, P. S., Burt, T. P. and Butcher, D. P. 1987. *Computer Simulation in Physical Geography*, J. Wiley & Sons, Chichester, 227 pp.
- Kubik, K. and Botman, A. G. 1976. 'Interpolation accuracy for topographic and geological surfaces', *ITC Journal*, **2**, 236–274.
- van Kuilenburg, J., de Gruijter, J. J., Marsman, B. A. and Bouma, J. 1982. 'Accuracy of spatial interpolation between point data on moisture supply capacity, compared with estimates from mapping units', *Geoderma*, **27**, 311–325.
- Lam, N. 1983. 'Spatial interpolation methods: a review', *The American Cartographer*, **10**(2), 129–149.
- Laslett, G. M., McBratney, A. B., Pahl, P. J. and Hutchinson, M. F. 1987. 'Comparison of several spatial prediction methods for soil pH', *Journal of Soil Science*, **38**, 325–241.
- Li, Z. 1988. 'On the measure of digital terrain model accuracy', *Photogrammetric Record*, **12**(72), 873–877.
- Li, Z. 1992. 'Variation of the accuracy of digital terrain models with sampling interval', *Photogrammetric Record*, **14**(79), 113–128.
- Li, Z. 1994. 'A comparative study of the accuracy of digital terrain models (DTMs) based on various data models', *ISPRS Journal of Photogrammetry and Remote Sensing*, **49**(1), 2–11.
- Meinguet, J. 1979. 'Multivariate interpolation at arbitrary points made simple', *Journal of Applied Mathematics and Physics*, **30**, 292–304.
- Miller, C. L. and Laflamme, R. A. 1958. 'The digital terrain model – theory and application', *Photogrammetric Engineering*, **24**(3), 433.
- Mitasova, H. and Mitas, L. 1993. 'Interpolation by regularized spline with tension. I. Theory and Implementation', *Mathematical Geology*, **25**, 641–655.
- Mitasova, H., Mitas, L., Brown, W. M., Gerdes, D. P., Kosinovsky, I. and Baker, T. 1995. 'Modelling spatially and temporally distributed phenomena: new methods and tools for GRASS GIS', *International Journal of Geographical Information Systems*, **9**(4), 433–446.
- Moore, I. D., Burch, G. J. and MacKenzie, D. H. 1988. 'Topographic effects on the distribution of surface soil water and the location of ephemeral gullies', *Transactions of the ASAE*, **31**(4), 1098–1107.
- Moore, I. D., Turner, A. K., Wilson, J. P., Jenson, S. K. and Band, L. E. 1993. 'GIS and land-surface-subsurface modeling', in Goodchild, M. F., Parks, B. O. and Steyaert, L. T. (Eds), *Environmental Modeling with GIS*, Oxford University Press, New York, 196–230.
- Moran, P. A. P. 1950. 'Notes on continuous stochastic phenomena', *Biometrika*, **37**, 17–23.
- Morris, D. G. and Heerdegen, R. G. 1988. 'Automatically derived catchment boundary and channel networks and their hydrological applications', *Geomorphology*, **1**, 131–141.
- Oliver, M. A. and Webster, R. 1990. 'Kriging: a method of interpolation for geographical information systems', *International Journal of Geographical Information Systems*, **4**(3), 313–332.
- Panuska, J. C., Moore, E. D. and Kramer, L. A. 1991. 'Terrain analysis: integration into the agricultural nonpoint source (AGNPS) pollution model', *Journal of Soil and Water Conservation*, **46**(1), 59–64.
- Petrie, G. 1990. 'Modelling, interpolation and contouring procedures', in Petrie, G. and Kennie, T. J. M. (Eds), *Terrain Modelling in Surveying and Civil Engineering*, Whittles Publishing Services, Caithness, 112–127.
- Rhind, D. W. 1975. 'A skeletal overview of spatial interpolation', *Computer Applications*, **2**(3–4), 293–309.
- SAS Institute. 1990. *SAS/GRAPH Software: Reference Version 6*, Sas Institute Inc., Cary NC, 1342 pp.
- Schut, G. H. 1976. 'Review of interpolation methods for digital terrain models', *The Canadian Surveyor*, **30**(5), 389–412.
- Torlegard, K., Östman, A. and Lindgren, R. 1986. 'A comparative test of photogrammetrically sampled digital elevation models', *Photogrammetria*, **41**, 1–16.
- Yoeli, P. 1983. 'Digital terrain models and their cartographic and cartometric utilisation', *The Cartographic Journal*, **20**(1), 17–22.
- Young, R. A., Onstad, C. A., Bosch, D. D. and Anderson, W. P. 1989. 'AGNPS: a nonpoint-source pollution model for evaluating agricultural watersheds', *Journal of Soil and Water Conservation*, **44**(2), 168–173.
- Zevenbergen, L. W. and Thorne, C. R. 1987. 'Quantitative analysis of land surface topography', *Earth Surface Processes and Landforms*, **12**, 47–56.